Vision Res. Vol. 33, No. 15, pp. 2113–2125, 1993
Printed in Great Britain.

0042-6989/93 $6.00 + 0.00

Functional Segregation of Color and Motion Perception Examined in Motion Nulling

EDUARDO-JOSÉ CHICHILNISKY,* DAVID HEEGER,* BRIAN A. WANDELL*

Received 14 December 1992; in revised form 3 January 1993

We examine two hypotheses about the functional segregation of color and motion perception, using a motion nulling task. The most common interpretation of functional segregation, that motion perception depends only on one of the three dimensions of color, is rejected. We propose and test an alternative formulation of functional segregation: that motion perception depends on a univariate motion signal driven by all three color dimensions, and that the motion signal is determined by the product of the stimulus contrast and a term that depends only on the relative cone excitations. Two predictions of this model are confirmed. First, motion nulling is transitive: when two stimuli null a third they also null another. Second, motion nulling is homogeneous: if two stimuli null one another, they continue to null one another when their contrasts are scaled equally. We describe how to apply our formulation of functional segregation to other behavioral and physiological measurements.

Functional segregation Color Motion nulling Motion energy Parallel pathways

INTRODUCTION

A variety of demonstrations and experiments illustrate that the contrast and color of a moving target influences its detection threshold, direction discrimination threshold, direction of movement, and perceived velocity (Carney, Shadlen & Switkes, 1987; Cavanagh, Tyler & Favreau, 1984; Cavanagh, MacLeod & Anstis, 1987; Lee & Stromeyer, 1989; Palmer, Mobley & Teller, 1993; Ramachandran & Gregory, 1978; Stone, Watson & Mulligan, 1990; Thompson, 1982). This codependence suggests a connection between the neural representations of color and motion. However, the additional psychophysical observation that weakening the luminance signal degrades or eliminates motion perception (Cavanagh *et al.*, 1984; Ramachandran & Gregory, 1978; Teller & Lindsey, 1993) has led some theorists to explore the opposite hypothesis: namely, that anatomically distinct brain nuclei mediate color and motion perception (Livingstone & Hubel, 1987; Meadows, 1974; Zeki, 1975, 1990, 1991; Zeki, Watson, Lueck, Friston & Frackowiack, 1991; Zihl, von Cramon & Mai, 1983). Zeki refers to this hypothesis as *functional segregation*.

Two separate difficulties plague attempts to couple luminance and functional segregation. First, the degraded motion percept at isoluminance does not demonstrate that motion perception only depends on the luminance dimension of color. To test this idea we must show that the other two dimensions of color fail to influence motion perception at all luminance levels.

Second, the luminance hypothesis needlessly restricts the idea of functional segregation. The privileged role of luminance in motion perception has been rejected (Cavanagh *et al.*, 1984; Cavanagh & Favreau, 1985; Cavanagh & Anstis, 1991; Derrington & Badcock, 1985; Kaiser, Vimal, Cowan & Hibino, 1989; Krauskopf & Farell, 1990; Lindsey & Teller, 1990; Logothetis, Schiller, Charles & Hurlbert, 1990; Mullen & Baker, 1985; Mullen & Boulton, 1992; Palmer *et al.*, 1993; Papathomas, Gorea & Julesz, 1991; Saito, Tanaka, Isono, Yasuda & Mikami, 1989; Webster, Day & Cassell, 1992). But other psychophysical formulations, not based on luminance, are consistent with functional segregation.

In this paper we frame and test hypotheses about the relationship between motion and the three dimensions of color. We use a motion nulling task (Cavanagh & Anstis, 1991) that includes a wide range of luminance and chromatic stimuli. We reject the most common interpretation of functional segregation: that motion nulling depends only on one of the three dimensions of color. We propose an alternative formulation of functional segregation: that the motion signal at each point in the visual field is a single time-varying number that is a nonlinear combination of cone signals. Since we require three variables to represent color, this *univariate* representation segregates motion from color.

Our experimental results are consistent with the existence of a univariate motion signal. Moreover, we find that the motion signal depends on the product of two terms. The first term depends only on the stimulus contrast; the second term depends only on the stimulus color, and thus provides a unique color signature for the motion signal. We discuss how to apply this color

*Department of Psychology, Stanford University, Jordan Hall, Building 420, Stanford, CA 94305, U.S.A.

signature to other behavioral and physiological measurements.

METHODS

Overview

Observers viewed foveally two vertical gratings drifting in opposite directions, superimposed on a uniform gray background. We call them the *test* and *nulling* gratings. The gratings had sinusoidal contrast profiles and different colors. We varied the contrast of the nulling grating and asked observers to indicate the perceived direction of motion of the composite stimulus.

We estimated the contrast of the nulling grating at which the subject was equally likely to report composite motion in the test or nulling direction. At this contrast, subjects perceived ambiguous motion or stationary, colored flicker. In this way we obtained a pair of gratings that each cancelled the motion percept generated by the other.

Stimuli

Observers sat in a dark room and viewed a color CRT screen 3 m away. The screen occupied 5 deg of the central field of view. Observers fixated a small black spot at the center of the screen that was present throughout the experiment. They adapted to a uniform gray screen of 57 cd/m^2 for about 1.5 min before beginning the trials. Following adaptation, pairs of moving gratings were presented in a circular region 1.5 deg in diameter in the center of the uniform field (1.0 deg for subject ES). The gratings always had a fixed spatial frequency of 1.33 c/deg (2 c/deg for subject ES). The gratings drifted in opposite directions at 2 Hz for 0.5 sec before being replaced by the the uniform gray background. We did not monitor fixation and we are certain that eye movements occurred during some trials.

We calculate the grating contrast seen by each receptor class (uncorrected for chromatic aberration) from the spectral composition of the grating and the spectral sensitivity of the human L, M, and S cones (Schnapf, Kraft & Baylor, 1987; Smith & Pokorny, 1975). Suppose the cone excitations at the peak and trough of the sinusoidal grating are $L_{\max}$ and $L_{\min}$. The L cone contrast is $l = (L_{\max} - L_{\min})/(L_{\max} + L_{\min})$. Defining the cone contrast for the M and S cones in the same way, we represent the grating using the cone contrast vector $\mathbf{a} = (l, m, s)$. We define the overall grating contrast as the magnitude of the cone contrast vector, $\|\mathbf{a}\| = \sqrt{l^2 + m^2 + s^2}$. Although this measure of contrast depends on the color space we use (i.e. the photoreceptors), our conclusions hold for any color space within a linear transformation of the receptors.

The color direction of the vector $\mathbf{a}$ is the unit length vector pointing in the same direction, $\mathbf{a}/\|\mathbf{a}\|$. Two vectors with the same color direction and different contrasts stimulate the cones in the same ratios.

To establish the contrast for a motion null, subjects judged 192 presentations of a test grating with a fixed color direction and contrast and a nulling grating with a different fixed color direction and variable contrast. The two gratings always moved in opposite directions, but which grating moved rightward was randomized on each trial. The subject reported the perceived direction of motion (left or right) of the composite by pressing a button. The nulling grating contrast was adjusted using a double random staircase procedure: when the subject's response coincided with the nulling grating direction, the nulling grating contrast was decreased; otherwise its contrast was increased. A new trial began shortly after the subject responded.

When the subject's judgments of motion direction are equally likely to follow the test grating **a** or the nulling grating **b**, we say that **b** nulls **a**. We use the notation $\mathbf{b} \sim \mathbf{a}$ to indicate a pair of stimuli that null one another. We say that **a** and **b** have the same *motion nulling strength*.

Our experiments included measurements using test gratings that stimulated all three photoreceptor classes in many ratios. The nulling gratings in Fig. 3 had zero S cone contrast, so they can be represented on a graph that plots the values of the L and M cone contrasts.

In our notation, the stimuli (l, m, s) and $(-l, -m, -s)$ represent the same grating in opposite phases. During a trial, the test and nulling gratings pass through all relative phases several times. The difference between (l, m, s) and $(-l, -m, -s)$ is only that they begin and end the trial shifted by one half cycle with respect to the test. When we used a nulling stimulus (l, m, s), we often repeated the measurement using $(-l, -m, -s)$. Unsurprisingly, we observed that these stimuli had the same motion nulling strength. Hence, when we make a measurement at (l, m, s) we also place a corresponding point at $(-l, -m, -s)$ on our graphs.

Subjective experience

The staircase procedure kept the test and nulling contrast near a motion equilibrium. At the equilibrium, subjects perceived a stimulus that appeared to be flickering or to have ambiguous motion. Most decisions, based on stimuli just to one side or the other of the equilibrium, were easy. But for some subjects and some combinations of test and nulling grating colors, there was a percept of two gratings slipping over one another. These conditions were infrequent but repeatable.

Estimating the nulling contrast

At the ith contrast level c_i of the nulling grating, the subject reported motion in the direction of the nulling grating in n_i out of a total of m_i trials. From these data, we estimated the probability $P(c_i)$ of seeing motion in the direction of the nulling grating at this contrast. We fitted a cumulative Gaussian function to the values $P(c_i)$, with contrast represented on a log scale, using a maximum likelihood method (Watson, 1979). From this fit, we estimated the contrast c of the nulling grating at which the subject was equally likely to report composite motion in either direction.

The cumulative Gaussian provided an adequate fit to the psychometric functions, as illustrated in Fig. 1. Here

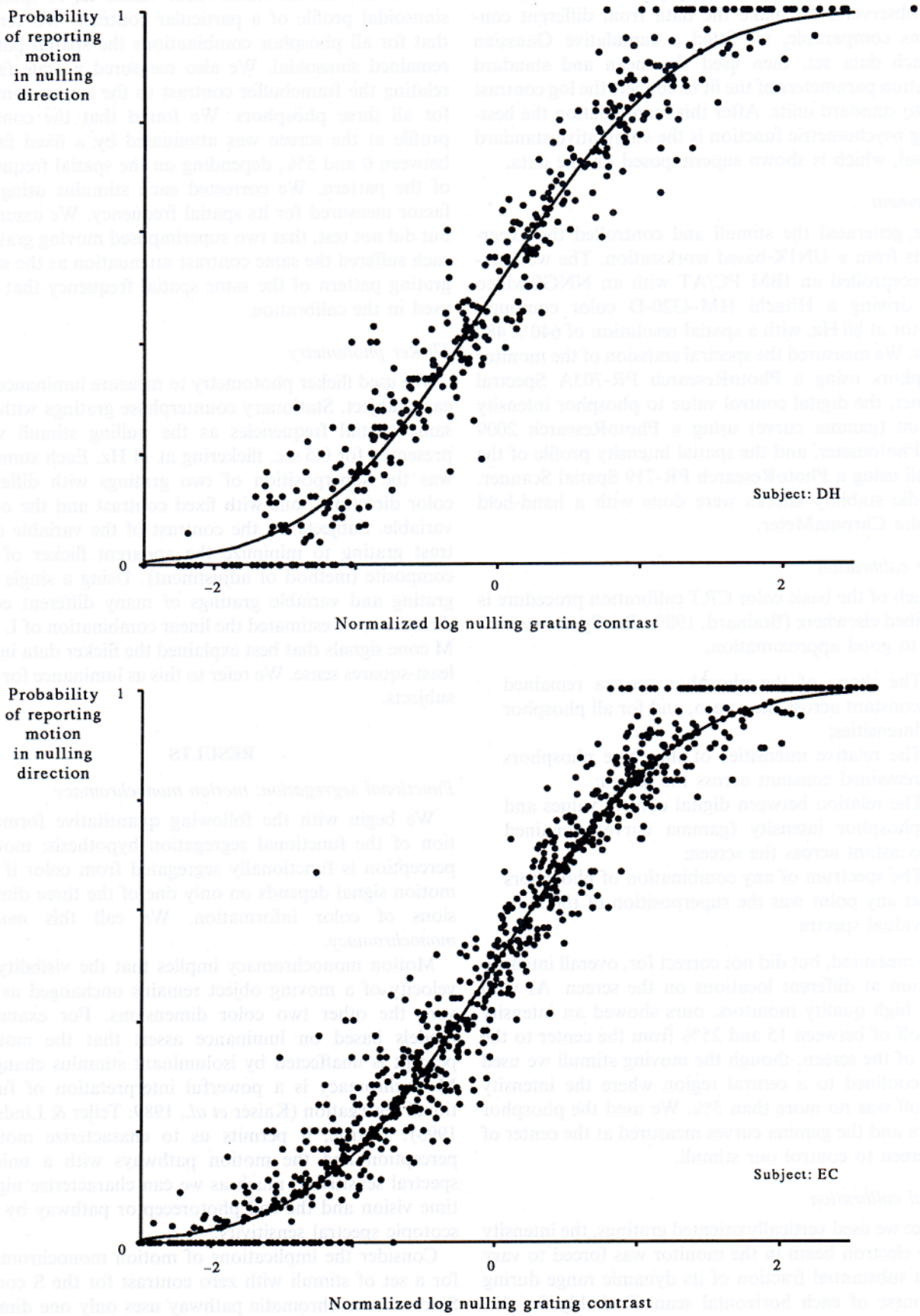

FIGURE 1. Cumulative Gaussian fits to psychometric functions. The probability of seeing motion in the nulling direction is plotted against the log contrast of the nulling grating. Data from many different experiments are superimposed. The log contrast axis of each individual data set was shifted and scaled by the mean and standard deviation parameters of the maximum likelihood cumulative Gaussian fit (Watson, 1979) in order to make different data sets comparable. The cumulative standard normal distribution is shown superimposed on the transformed data.

we have superimposed all the psychometric data from two observers. To make the data from different conditions comparable, we fitted a cumulative Gaussian to each data set, then used the mean and standard deviation parameters of the fit to convert the log contrast axis to standard units. After this manipulation the best-fitting psychometric function is the cumulative standard normal, which is shown superimposed on the data.

Equipment

We generated the stimuli and controlled the experiments from a UNIX-based workstation. The workstation controlled an IBM PC/AT with an NNGS video card driving a Hitachi HM-4320-D color computer monitor at 88 Hz, with a spatial resolution of 640 × 480 pixels. We measured the spectral emission of the monitor phosphors using a PhotoResearch PR-703A Spectral Scanner, the digital control value to phosphor intensity relation (gamma curve) using a PhotoResearch 2009 Tele-Photometer, and the spatial intensity profile of the stimuli using a PhotoResearch PR-719 Spatial Scanner. Periodic stability checks were done with a hand-held Minolta ChromaMeter.

Color calibration

Much of the basic color CRT calibration procedure is described elsewhere (Brainard, 1989). Briefly, we verified that, to good approximation,

- The shape of the phosphor spectra remained constant across the screen, and for all phosphor intensities;
- The relative intensities of the three phosphors remained constant across the screen;
- The relation between digital control values and phosphor intensity (gamma curve) remained constant across the screen;
- The spectrum of any combination of phosphors at any point was the superposition of the individual spectra.

We measured, but did not correct for, overall intensity variation at different locations on the screen. As with many high quality monitors, ours showed an intensity drop-off of between 15 and 25% from the center to the edges of the screen, though the moving stimuli we used were confined to a central region where the intensity drop-off was no more than 5%. We used the phosphor spectra and the gamma curves measured at the center of the screen to control our stimuli.

Spatial calibration

Since we used vertically oriented gratings, the intensity of the electron beam in the monitor was forced to vary over a substantial fraction of its dynamic range during the course of each horizontal scan. Probably for this reason, the actual contrast of a spatial pattern on the screen was slightly different from the contrast specified according to the point-by point calibrations described above.

We measured the stimulus pattern that appeared on the screen with the framebuffer values set to specify a sinusoidal profile of a particular contrast. We verified that for all phosphor combinations the spatial pattern remained sinusoidal. We also measured a scale factor relating the framebuffer contrast to the screen contrast for all three phosphors. We found that the contrast profile at the screen was attenuated by a fixed factor between 0 and 5%, depending on the spatial frequency of the pattern. We corrected each stimulus using the factor measured for its spatial frequency. We assumed, but did not test, that two superimposed moving gratings each suffered the same contrast attenuation as the static grating pattern of the same spatial frequency that was used in the calibration.

Flicker photometry

We used flicker photometry to measure luminance for each subject. Stationary counterphase gratings with the same spatial frequencies as the nulling stimuli were presented for 0.5 sec, flickering at 11 Hz. Each stimulus was the superposition of two gratings with different color directions, one with fixed contrast and the other variable. Subjects set the contrast of the variable contrast grating to minimize the apparent flicker of the composite (method of adjustment). Using a single test grating and variable gratings of many different color directions, we estimated the linear combination of L and M cone signals that best explained the flicker data in the least-squares sense. We refer to this as luminance for our subjects.

RESULTS

Functional segregation: motion monochromacy

We begin with the following quantitative formulation of the functional segregation hypothesis: motion perception is functionally segregated from color if the motion signal depends on only one of the three dimensions of color information. We call this *motion monochromacy*.

Motion monochromacy implies that the visibility or velocity of a moving object remains unchanged as we vary the other two color dimensions. For example, models based on luminance assert that the motion percept is unaffected by isoluminant stimulus changes. Monochromacy is a powerful interpretation of functional segregation (Kaiser *et al.*, 1989; Teller & Lindsey, 1993). If true, it permits us to characterize motion perception and the motion pathways with a unique spectral sensitivity, much as we can characterize nighttime vision and the rod photoreceptor pathway by the scotopic spectral sensitivity.

Consider the implications of motion monochromacy for a set of stimuli with zero contrast for the S cones. Since a monochromatic pathway uses only one dimension of color, stimuli with equal motion nulling strength should fall along straight lines, as depicted in Fig. 2. These lines should be perpendicular to the color dimension responsible for motion perception. For example, models based on luminance demand that stimuli with

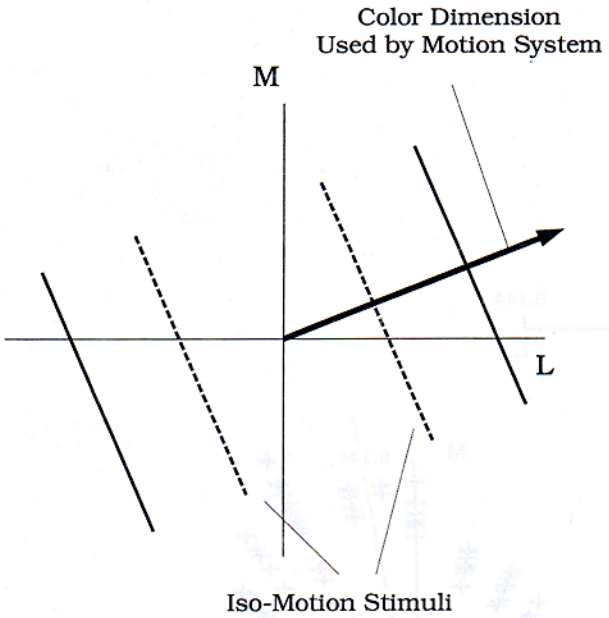

FIGURE 2. Monochromatic theory predictions. Suppose only one dimension of color controls motion perception. Then stimuli with equal motion strength that do not stimulate the S cones should fall on parallel lines symmetric about the origin, when plotted according to their L and M cone contrast. The lines are orthogonal to the color direction responsible for motion perception.

equal motion nulling strength should fall on isoluminant lines (Teller & Lindsey, 1993).

Figure 3 plots the L and M cone contrasts of many gratings that all null the same test grating. These gratings all have the same motion nulling strength. Since the data do not fall on parallel lines, motion nulling strength does not depend on a single color dimension. We reject motion monochromacy in this task.

Functional segregation: Stiles color invariance

Now we consider an alternate formulation of functional segregation. We suppose that the motion signal at each point in the visual field is a single time-varying number. Since we require three variables to represent color, this *univariate* representation segregates motion from color. We will see later that our experiments are consistent with a univariate representation.

We now investigate the specific hypothesis that the motion signal from a stimulus **a** is monotonically related to the product of two terms, the stimulus contrast and a sensitivity term that depends only on the stimulus color direction:

$$\|\mathbf{a}\| S(\mathbf{a}/\|\mathbf{a}\|).$$

In this case we say that the motion signal obeys *Stiles color invariance*.*

Our formulation removes the restriction, which is plainly too strong, that luminance or any single color dimension is the sole carrier of the motion signal (Cavanagh *et al.*, 1984; Cavanagh & Favreau, 1985; Cavanagh & Anstis, 1991; Derrington & Badcock, 1985; Kaiser *et al.*, 1989; Krauskopf & Farell, 1990; Lindsey & Teller, 1990; Logothetis *et al.*, 1990; Mullen & Baker, 1985; Mullen & Boulton, 1992; Palmer *et al.*, 1993; Papathomas *et al.*, 1991; Saito *et al.*, 1989; Webster *et al.*, 1992). But the univariate signal preserves the segregation of the color and motion computations. Finally, Stiles invariance allows us to define the color direction sensitivity, S, to serve as a color signature for identifying the motion signal in a variety of contexts.

A test of Stiles invariance: homogeneity

We tested Stiles invariance in motion nulling using the following logic. Stiles invariance means that the motion nulling strength of a stimulus, **a**, depends on the product of its contrast $\|\mathbf{a}\|$, and a color direction sensitivity term, $S(\mathbf{a}/\|\mathbf{a}\|)$. This implies that if two gratings null one another, they will continue to null each other when we scale their contrasts equally. That is, if $\mathbf{a} \sim \mathbf{b}$, then $\|\mathbf{a}\| S(\mathbf{a}/\|\mathbf{a}\|) = \|\mathbf{b}\| S(\mathbf{b}/\|\mathbf{b}\|)$ so $\|k\mathbf{a}\| S(k\mathbf{a}/\|k\mathbf{a}\|) = \|k\mathbf{b}\| S(k\mathbf{b}/\|k\mathbf{b}\|)$, and $k\mathbf{a} \sim k\mathbf{b}$. We call this property *homogeneity*.

We examined Stiles invariance by testing homogeneity in motion nulling. We show the results of these tests in Figs 4 and 5. In each panel of Fig. 4, we plot the contrast of nulling gratings vs the contrast of test gratings they nulled. Within a panel the color directions of the test and nulling gratings are fixed, but different from one another. Different panels show measurements using various color directions of the test and nulling gratings.

We summarize our homogeneity tests in Fig. 5. We have superimposed many data sets like those in Fig. 4 after rescaling the axes of each panel so that the best-fitting line has unit slope. The points fall close to the identity lines shown as required by homogeneity.

For subject EC, we used repeated measurements in four pairs of color directions to test homogeneity statistically. A χ^2-test on the residuals failed to reject homogeneity ($P = 0.31$). Our data support homogeneity.

Transitivity

Our experimental analyses are based on the premise that $\mathbf{a} \sim \mathbf{b}$ means that **a** and **b** have the same motion nulling strength. This inference only makes sense if $\mathbf{a} \sim \mathbf{b}$ and $\mathbf{b} \sim \mathbf{c}$ implies that $\mathbf{a} \sim \mathbf{c}$. We call this property *transitivity*.

To test transitivity, we measured the contrast of grating **b** required to null a test grating **a**, resulting in a measurement $\mathbf{a} \sim s\mathbf{b}$. Similarly we obtained a measurement $\mathbf{b} \sim r\mathbf{c}$. From homogeneity, we know that $s\mathbf{b} \sim (sr)\mathbf{c}$, and by transitivity we expect that $\mathbf{a} \sim (sr)\mathbf{c}$. We tested this prediction by having the subject cancel **a** by adjusting the contrast of **c**, yielding a measurement $\mathbf{a} \sim q\mathbf{c}$. Transitivity predicts that the $q = sr$. Figure 6 contains a histogram of $\log(q/sr)$ for many choices of color directions **a**, **b**, and **c**.

The superimposed dotted line shows a Gaussian distribution that we predicted from the variability of repeated measurements, using the following logic. There are three measurements for each transitivity test, q, r, and s. If

*The brilliant color scientist, W. S. Stiles, used this empirical property to define the spectral sensitivity of the mechanisms of light adaption in the human visual system (Stiles, 1939, 1959, 1978).

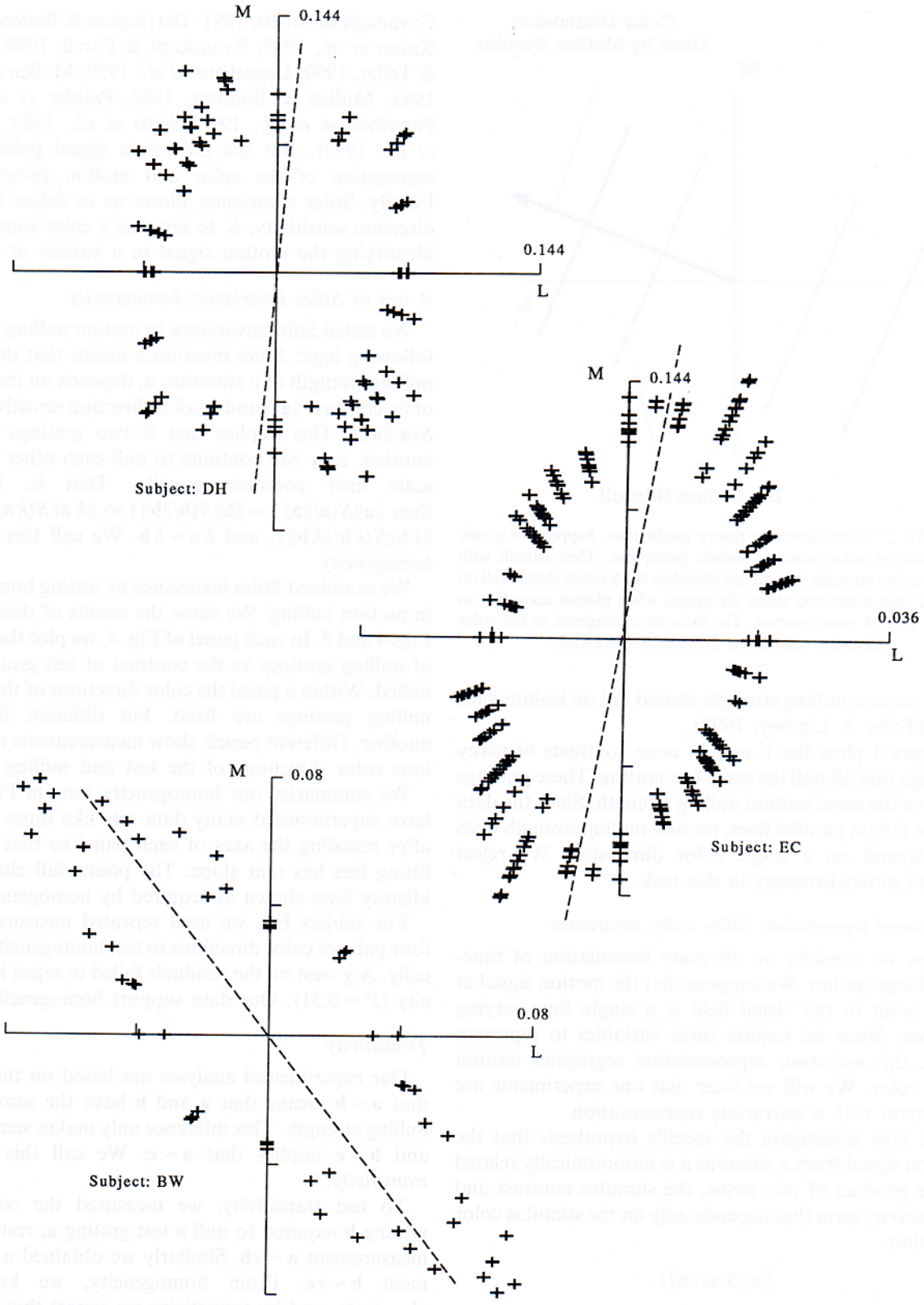

FIGURE 3. Many gratings that nulled a single test, for three observers. Each point represents the L and M cone contrast of a nulling grating that cancelled the motion of a standard test grating (S cones contrasts are zero for these nulling gratings). The cone contrasts of the test gratings for each subject are: BW (0.017, 0.028, 0.159), DH (0.059, 0.097, 0.535), EC (0.024, 0.04, 0.225). Each nulling stimulus is plotted on both sides of the origin, because antipodal points represent stimuli that are identical up to a phase shift, and have the same effect in motion nulling. The dashed lines are isoluminant lines, measured using flicker photometry (data not shown). The iso-motion contours and luminance measurements differ between subjects: subjects do not accept each other's motion nulls or minimum flicker settings. For two observers the isoluminant line falls nearly along the M cone axis, indicating little or no M cone contribution to luminance. These observers' luminance settings fall within the range of settings made by Gibson and Tyndall's (1923) observers. Those data define the CIE standard luminous efficiency function in the wavelength region relevant to our measurements (Wyszecki & Stiles, 1982).

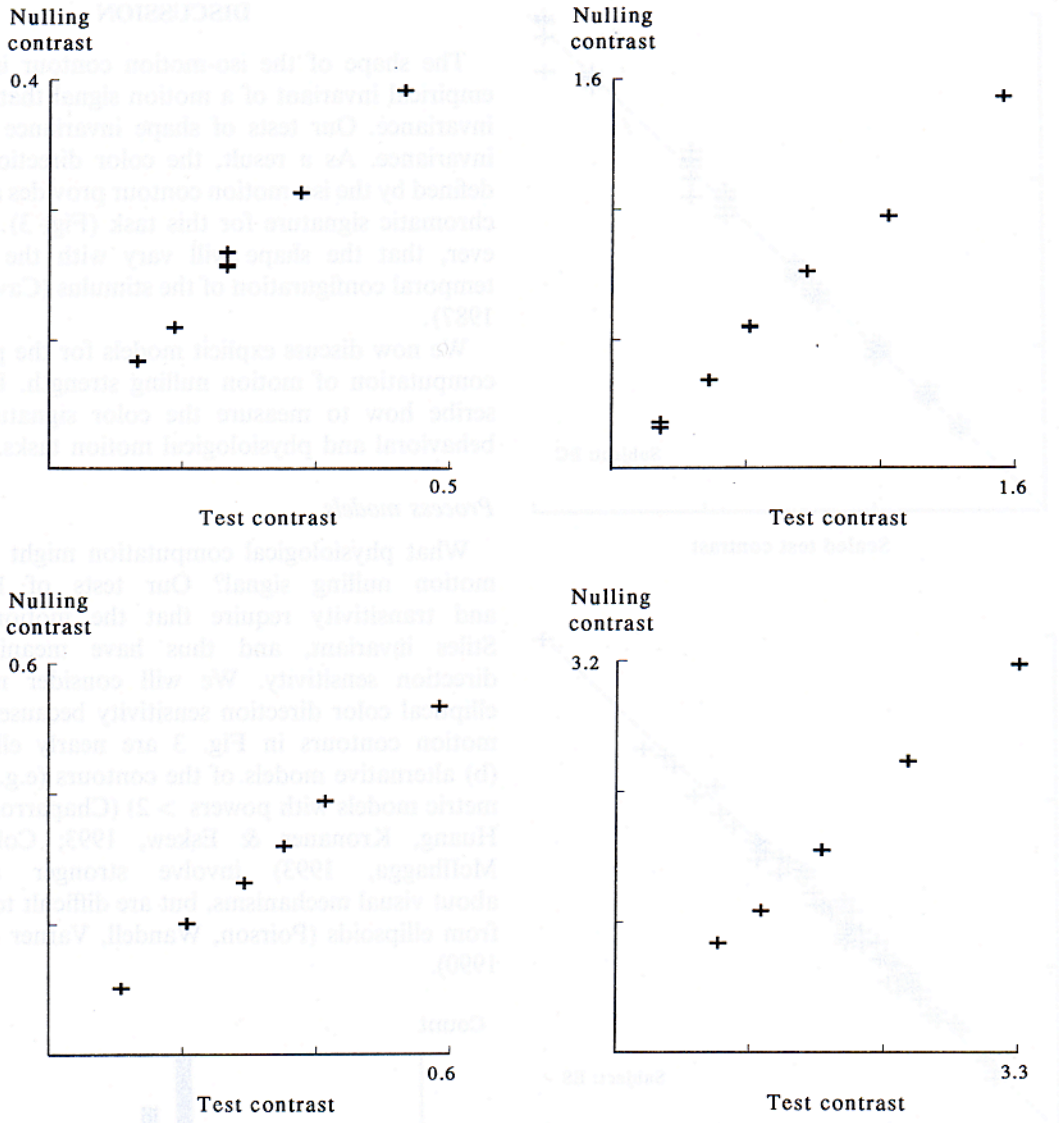

FIGURE 4. Tests of homogeneity for one observer. Each panel is a test of homogeneity for a different choice of test and nulling color directions. Within each panel, the test and nulling color directions are fixed but different. The points depict the measured contrast of the nulling grating as a function of the test contrast. Homogeneity predicts that all the points in each panel should lie on a straight line through the origin.

transitivity holds precisely, $\log(q/sr) = 0$. Assuming that $\log(s)$, $\log(r)$, and $\log(q)$ are each subject to independent additive noise with variance σ^2, the quantity $\log(q/sr) = \log(q) - \log(s) - \log(r)$ should have variance $3\sigma^2$. We generated an estimate $\hat{\sigma}^2$ for σ^2 from repeated nulling measurements in many color directions. The Gaussian distribution superimposed on the data in Fig. 6 has variance $3\hat{\sigma}^2$. This curve adequately predicts the measured variability in $\log(q/sr)$, consistent with transitivity. We conclude that our data are consistent with the existence of a univariate motion strength signal.

The color direction sensitivity

We refer to the closed curve traced out by each data set in Fig. 3 as an *iso-motion contour*. Transitivity and homogeneity together imply that the shape is independent of the contrast and color direction of the test stimulus.

To show this, suppose we measure the contrast of stimulus **a** required to null stimulus **b**, resulting in a measurement $k\mathbf{a} \sim \mathbf{b}$. How will the set of stimuli that null **a** be related to the set of stimuli that null **b**? If $\mathbf{c} \sim \mathbf{a}$, then by homogeneity $k\mathbf{a} \sim k\mathbf{c}$, and by transitivity, $\mathbf{b} \sim k\mathbf{c}$. This proves that if $\mathbf{a} \sim \mathbf{c}$, then $\mathbf{b} \sim k\mathbf{c}$. The stimuli that cancel **a** and **b** are the same except for a single scale factor, k, so the two contours have the same shape.

We tested this prediction directly. Each large panel in Fig. 7 shows many nulling stimuli that cancelled a single test stimulus. The test stimuli in the two panels were very

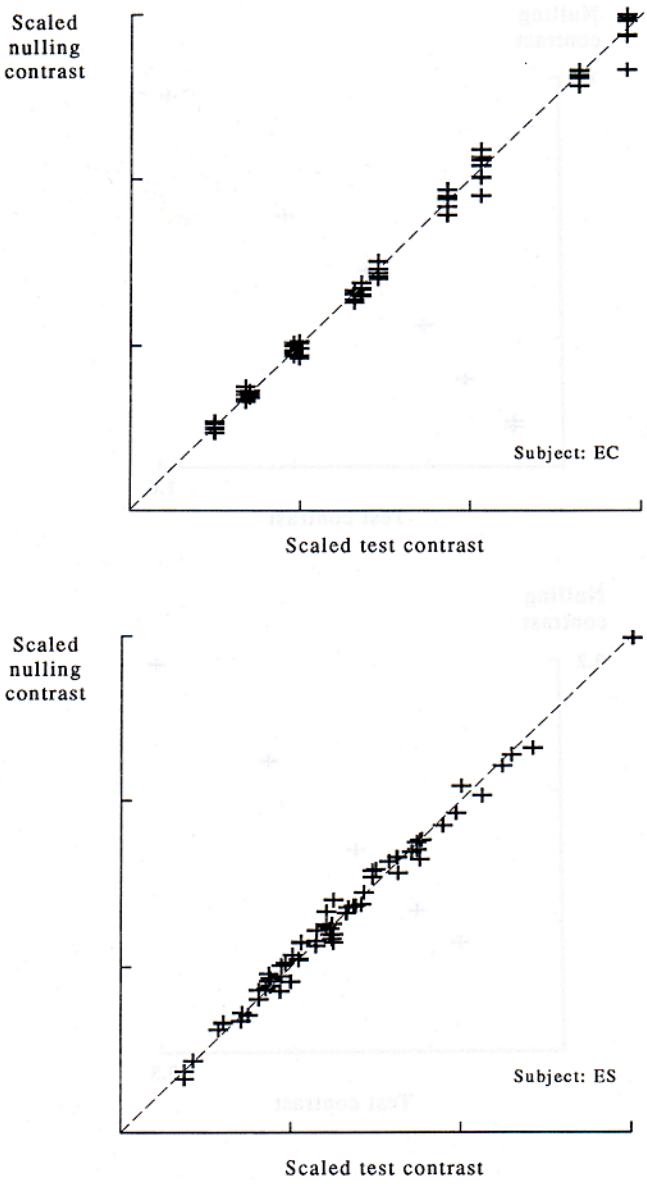

FIGURE 5. Summarized test of homogeneity for two observers. Each panel is a summarized test of homogeneity for one observer. We gathered many data sets like those in Fig. 4 and rescaled the axes of each plot so that the best-fitting line had unit slope. We then superimposed these data sets for each observer. Homogeneity predicts these data should fall on the 45 deg diagonal lines shown.

different: one is a saturated blue–yellow pattern and the other a moderate white–black. The second test stimulus produced increased nulling contrast variability in certain color directions. Still, the iso-motion contours defined by the average nulling contrasts have the same shape, as predicted by homogeneity and transitivity.

This is detailed in the inset panel. For 11 different nulling color directions, we plot the difference between the mean log nulling contrast measured with the blue–yellow and white–black test stimuli. If the two iso-motion contours have the same shape, these differences should be the same for all nulling color directions. The measurements fall near the best-fitting constant value of 0.246.

DISCUSSION

The shape of the iso-motion contour is the crucial empirical invariant of a motion signal that obeys Stiles invariance. Our tests of shape invariance imply Stiles invariance. As a result, the color direction sensitivity defined by the iso-motion contour provides a meaningful chromatic signature for this task (Fig. 3). Note, however, that the shape will vary with the spatial and temporal configuration of the stimulus (Cavanagh *et al.*, 1987).

We now discuss explicit models for the physiological computation of motion nulling strength. Later we describe how to measure the color signature of other behavioral and physiological motion tasks.

Process models

What physiological computation might produce the motion nulling signal? Our tests of homogeneity and transitivity require that the motion signal be Stiles invariant, and thus have meaningful color direction sensitivity. We will consider models with elliptical color direction sensitivity because (a) the iso-motion contours in Fig. 3 are nearly elliptical, and (b) alternative models of the contours (e.g. Minkowski metric models with powers > 2) (Chaparro, Stromeyer, Huang, Kronauer & Eskew, 1993; Cole, Hine & McIlhagga, 1993) involve stronger assumptions about visual mechanisms, but are difficult to distinguish from ellipsoids (Poirson, Wandell, Varner & Brainard, 1990).

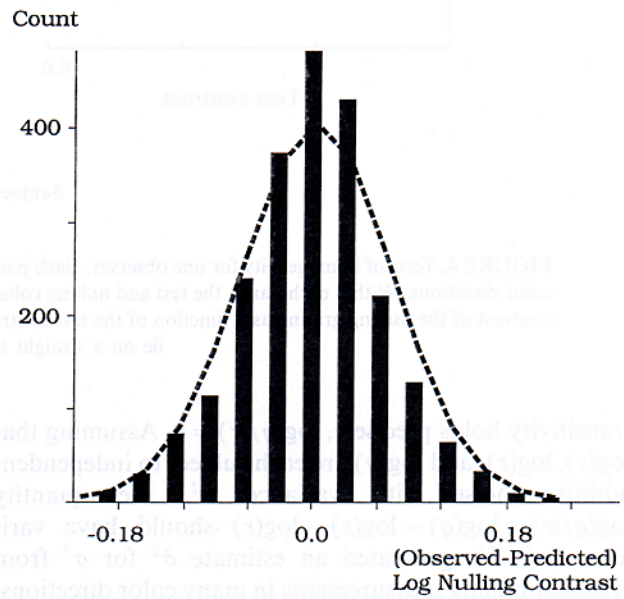

FIGURE 6. Test of transitivity for one observer. The histogram summarizes deviations from transitivity for one observer. Each datum contributing to the histogram is the log of the ratio of a measured nulling contrast to the contrast predicted from two other measurements, assuming transitivity and homogeneity. The data represent measurements in 13 different color directions; the large histogram counts reflect many predictions arising from all combinations of repeated measurements. The smooth curve is the expected distribution of the deviations based on the variability of repeated measurements. See text for details.

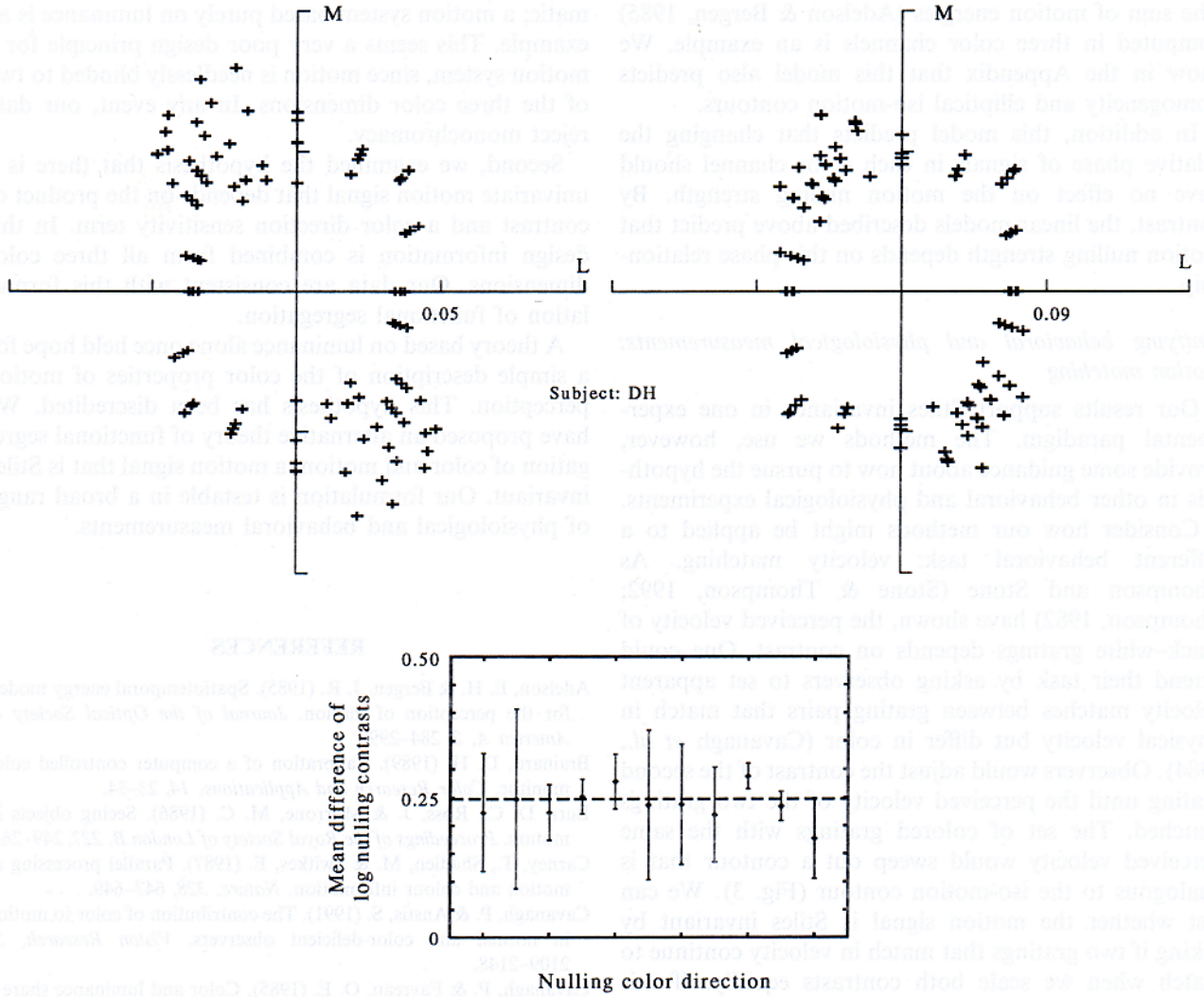

FIGURE 7. Homogeneity and transitivity for one observer. Each large panel depicts the L and M cone contrasts of many nulling gratings that cancel a single test grating. The test stimuli used in the two panels have cone contrasts (0.059, 0.097, 0.535) and (0.04, 0.022, 0.0) respectively. Their color appearances are roughly blue–yellow and white–black respectively. Transitivity and homogeneity together predict that the shape of the data sets in the two panels should be the same. The small inset panel plots the difference between the mean log nulling contrast measured with the blue–yellow and white–black test stimuli, for eleven different nulling color directions. Error bars represent two standard errors of the mean. See text for details.

Linear combination of delayed receptor signals. Our first model is a simple extension of the monochromacy hypothesis. We assume that motion nulling strength is the amplitude of the sum of the three delayed sinusoidal photoreceptor signals. When the delays for the different receptor classes are identical, this hypothesis is no more than the failed monochromacy hypothesis. If there is a relative delay between the different photoreceptor signals (Cavanagh & Anstis, 1991) then the amplitude of the combined signal is the square root of a quadratic function of the amplitudes of the photoreceptor signals (see Appendix). Therefore, this model predicts elliptical motion nulling contours whose precise shapes depend on the relative delays between the photoreceptor signals.

As we show in the Appendix, the delays between the L and M cone signals required to fit the data from the three observers in Fig. 3 are 46, 118, and 154 msec. These delays are comparable to the entire duration of human cone flash responses (Schnapf, Kraft & Baylor, 1987). Differential delays of this magnitude between the receptor signals are unlikely (Hamer & Tyler, 1992).

Linear combination of delayed color channels. A slightly more general model assumes that the photoreceptor signals are linearly recombined into three color channels (e.g. color-opponent channels). The outputs of the color channels are differentially delayed and added. Motion nulling strength is the amplitude of this sum.

This model also predicts an elliptical iso-motion contour (see Appendix). The dimensions and orientation are determined by the color transformation and the delays. We show in the Appendix that the delays and color transformation are confounded, making it impossible to assess the plausibility of the delays in this model without reference to a specific color transformation.

Quadratic combination of color channels. An alternative model postulates a quadratic combination rule: the motion nulling strength depends on the weighted sum of the squared amplitudes of signals in three color channels.

The sum of motion energies (Adelson & Bergen, 1985) computed in three color channels is an example. We show in the Appendix that this model also predicts homogeneity and elliptical iso-motion contours.

In addition, this model predicts that changing the relative phase of signals in each color channel should have no effect on the motion nulling strength. By contrast, the linear models described above predict that motion nulling strength depends on this phase relationship.

Unifying behavioral and physiological measurements: motion matching

Our results support Stiles invariance in one experimental paradigm. The methods we use, however, provide some guidance about how to pursue the hypothesis in other behavioral and physiological experiments.

Consider how our methods might be applied to a different behavioral task: velocity matching. As Thompson and Stone (Stone & Thompson, 1992; Thompson, 1982) have shown, the perceived velocity of black–white gratings depends on contrast. One could extend their task by asking observers to set apparent velocity matches between grating pairs that match in physical velocity but differ in color (Cavanagh *et al.*, 1984). Observers would adjust the contrast of the second grating until the perceived velocity of the two gratings matched. The set of colored gratings with the same perceived velocity would sweep out a contour that is analogous to the iso-motion contour (Fig. 3). We can test whether the motion signal is Stiles invariant by asking if two gratings that match in velocity continue to match when we scale both contrasts equally. If this quantitative test holds, then we can further ask whether the contour we derive from the experiment is the same as the contour we derive from the motion nulling experiment. The results of Cavanagh *et al.* (1984) are inconsistent with ellipsoidal contours, but they do not test Stiles invariance.

Next, consider how our methods might be applied to a physiological measurement: responses of single neurons in candidate motion areas. One would measure response as a function of contrast for many stimulus color directions, and test whether plots of response vs log contrast are horizontally shifted replicas. If so, the neuron's responses satisfy homogeneity, consistent with Stiles invariance. The size of the horizontal shift for each color direction defines a color direction sensitivity for the neuron analogous to behavioral iso-motion contours.

CONCLUSIONS

How can behavioral measurements address the physiological hypothesis of functional segregation between motion and color? We have argued that functional segregation is not properly tested by searching for a performance minimum at isoluminance.

Instead, we have considered two alternative formulations of functional segregation. First, we considered the hypothesis that motion perception is monochromatic; a motion system based purely on luminance is an example. This seems a very poor design principle for a motion system, since motion is needlessly blinded to two of the three color dimensions. In any event, our data reject monochromacy.

Second, we examined the hypothesis that there is a univariate motion signal that depends on the product of contrast and a color direction sensitivity term. In this design information is combined from all three color dimensions. Our data are consistent with this formulation of functional segregation.

A theory based on luminance alone once held hope for a simple description of the color properties of motion perception. This hypothesis has been discredited. We have proposed an alternative theory of functional segregation of color and motion: a motion signal that is Stiles invariant. Our formulation is testable in a broad range of physiological and behavioral measurements.

REFERENCES

Adelson, E. H. & Bergen, J. R. (1985). Spatiotemporal energy models for the perception of motion. *Journal of the Optical Society of America A*, *2*, 284–299.

Brainard, D. H. (1989). Calibration of a computer controlled color monitor. *Color Research and Applications*, *14*, 23–34.

Burr, D. C., Ross, J. & Morrone, M. C. (1986). Seeing objects in motion. *Proceedings of the Royal Society of London B*, *227*, 249–265.

Carney, T., Shadlen, M. & Switkes, E. (1987). Parallel processing of motion and colour information. *Nature*, *328*, 647–649.

Cavanagh, P. & Anstis, S. (1991). The contribution of color to motion in normal and color-deficient observers. *Vision Research*, *31* 2109–2148.

Cavanagh, P. & Favreau, O. E. (1985). Color and luminance share a common motion pathway. *Vision Research*, *25*, 685–688.

Cavanagh, P., MacLeod, D. & Anstis, S. (1987). Equiluminance: Spatial and temporal factors and the contribution of blue-sensitive cones. *Journal of the Optical Society of America A*, *4*, 1428–1438.

Cavanagh, P., Tyler, C. W. & Favreau, O. E. (1984). Perceived velocity of moving chromatic gratings. *Journal of the Optical Society of America A*, *1*, 893–899.

Chaparro, A., Stromeyer, C. S., Huang, E., Kronauer, R. & Eskew, R. E. Jr (1993). Colour is what the eye sees best. *Nature*, *361*, 348–350.

Cole, G. R., Hine, T. & McIlhagga, W. (1993). Detection mechanisms in l-, m- and s-cone contrast space. *Journal of the Optical Society of America*, *10*, 38–51.

Derrington, A. & Badcock, D. (1985). The low-level motion system has both chromatic and luminance input. *Vision Research*, *25*, 1879–1884.

Fahle, M. & Poggio, T. (1981). Visual hyperacuity: Spatiotemporal interpolation in human vision. *Proceedings of the Royal Society of London B*, *213*, 451–477.

Gibson, K. & Tyndall, E. (1923). Visibility of radiant energy. *Bulletin of the Bureau of Standards*, *19*, 131.

Hamer, R. & Tyler, C. (1992). Analysis of visual modulation sensitivity. V. faster visual response for g- than for r-cone pathway? *Journal of the Optical Society of America A*, *9*, 1889–1904.

Kaiser, P., Vimal, R., Cowan, W. & Hibino, H. (1989). Nulling of apparent motion as a method for assessing sensation luminance: An additivity test. *Color Research and Applications*, *14*, 187–191.

Krauskopf, J. & Farell, B. (1990). Influence of colour on the perception of coherent motion. *Nature*, *348*, 328–329.

Lee, J. & Stromeyer, C. F. III (1989). Contribution of human short-wave cones to luminance and motion detection. *Journal of Physiology*, *413*, 563–593.

Lindsey, D. T. & Teller, D. Y. (1990). Motion at isoluminance: Discrimination/detection ratios for moving isoluminant gratings. *Vision Research, 30*, 1751–1761.

Livingstone, M. S. & Hubel, D. H. (1987). Psychophysical evidence for separate channels for the perception of form, color, movement, and depth. *Journal of Neuroscience, 7*, 3416–3468.

Logothetis, N., Schiller, P., Charles, E. & Hurlbert, A. (1990). Perceptual deficits and activity of the color-opponent and broad-band pathways at isoluminance. *Science, 247*, 214–217.

Meadows, J. (1974). Disturbed perception of colours associated with localized cerebral lesions. *Brain, 97*, 615–632.

Mullen, K. T. & Baker, C. L. (1985). A motion aftereffect from an isoluminant stimulus. *Vision Research, 25*, 1595–1601.

Mullen, K. T. & Boulton, J. C. (1992). Absence of smooth motion perception in color vision. *Vision Research, 32*, 483–488.

Palmer, J., Mobley, L. & Teller, D. (1993). Motion at isoluminance: Discrimination/detection ratios and the summation of luminance and chromatic signals. *Journal of the Optical Society of America A*. In press.

Papathomas, T. V., Gorea, A. & Julesz, B. (1991). Two carriers for motion perception: Color and luminance. *Vision Research, 31*, 1883–1892.

Poirson, A. B., Wandell, B. A., Varner, D. & Brainard, D. H. (1990). Surface characterizations of color thresholds. *Journal of the Optical Society of America, 7*, 783–789.

Ramachandran, V. S. & Gregory, R.L. (1978). Does colour provide an input to human motion perception? *Nature, 275*, 55–56.

Saito, H., Tanaka, K., Isono, H., Yasuda, M. & Mikami, A. (1989). Directionally selective response of cells in the middle temporal area (MT) of the macaque monkey to the movement of equiluminous opponent color stimuli. *Experimental Brain Research, 75*, 1–14.

Schnapf, J. L., Kraft, T. W. & Baylor, D. A. (1987). Spectral sensitivity of human cone photoreceptors. *Nature, 325*, 439–441

Smith, V. & Pokorny, J. (1975). Spectral sensitivity of the foveal cone photopigments between 400 and 500 nm. *Vision Research, 15*, 161–171.

Stiles, W. S. (1939). The directional sensitivity of the retina and the spectral sensitivities of the rods and cones. *Proceedings of the Royal Society of London B, 127*, 64–105.

Stiles, W. S. (1959). Color vision: The approach through increment-threshold sensitivity. *Proceedings of the National Academy of Sciences U.S.A., 45*, 100–114.

Stiles, W. S. (1978). In *Mechanisms of colour vision*. London: Academic Press.

Stone, L. S. & Thompson, P. (1992). Human speed perception is contrast dependent. *Vision Research, 32*, 1535–1549.

Stone, L. S., Watson, A. B. & Mulligan, J. B. (1990). Effect of contrast on the perceived direction of a moving plaid. *Vision Research, 30*, 1049–1067.

Teller, D. & Lindsey, D. (1993). Motion at isoluminance: Motion dead zones in three-dimensional color space. *Journal of the Optical Society of America A*. In press.

Thompson, P. (1982). Perceived rate of movement depends on contrast. *Vision Research, 22*, 377–380.

Watson, A. B. (1979). Probability summation over time. *Vision Research, 19*, 515–522.

Watson, A. B. & Ahumada, A. J. (1983). A look at motion frequency domain. In Tsotsos, J. K. (ed.), *Motion: Perception and representation* (pp. 1–10). New York: Association for Computing Machinery.

Watson, A. B. & Ahumada, A. J. (1985). Model of human visual-motion sensing. *Journal of the Optical Society of America A, 2*, 322–342.

Webster, W., Day, R. & Cassell, J. (1992). Two movement aftereffects: Evidence for luminance- and color-movement pathways. *Vision Research, 32*, 2187–2190.

Wyszecki, G. & Stiles, W. S. (1982). *Color science* (2nd edn). New York: Wiley.

Zeki, S. (1975). The functional organization of projections from striate to prestriate visual cortex in the rhesus monkey. *Cold Spring Harbor Symposium on Quantitative Biology, 40*, 591–600.

Zeki, S. (1990). A century of cerebral achromatopsia. *Brain, 113*, 1721–1777.

Zeki, S. (1991). Cerebral akinetopsia (visual motion blindness). *Brain, 114*, 811–824.

Zeki, S., Watson, J., Leuck, C., Friston, K. & Frackowiak, R. (1991). A direct demonstration of functional specialization in human visual cortex. *Journal of Neuroscience, 11*, 641–649.

Zihl, J., von Cramon, D. & Mai, N. (1983). Selective disturbance of movement vision after bilateral brain damage. *Brain, 106*, 313–340.

Acknowledgements—We thank R. Fernald, S. du Lac, and W. Newsome for their comments on the manuscript, and L. Stone for valuable discussions. A preliminary version of this work was presented at the 1992 meeting of the Association for Research in Vision and Ophthalmology. This research was supported by National Eye Institute contract RO1 EY03164, NASA-Ames contract NCC2-307. E. J. Chichilnisky was supported by a predoctoral fellowship from the Howard Hughes Medical Institute.

APPENDIX

Linear combination of delayed receptor signals

Ellipsoidal iso-motion contours. Suppose the motion signal strength is the amplitude of the sum of differentially delayed receptor signals. In this case, the iso-motion contours are ellipsoidal.

The time-varying excitation patterns of the three photoreceptor classes in response to a single drifting grating stimulus are given by

$$L(x, t) = l \sin(x + t)$$

$$M(x, t) = m \sin(x + t)$$

$$S(x, t) = s \sin(x + t)$$

where the vector (l, m, s) is the color vector we have previously used to describe the stimulus. For simplicity, we have assumed unit spatial and temporal frequencies. Suppose the motion strength is the amplitude of the weighted sum of delayed receptor signals:

$$P = \|\omega_l l \sin(x + (t - d_l)) + \omega_m m \sin(x + (t - d_m)) + \omega_s s \sin(x + (t - d_s))\|$$

where $\|\cdot\|$ denotes the amplitude of the resulting sinusoidal signal. Applying trigonometric addition formulae and simplifying, we have

$$P^2 = \omega_l^2 l^2 + \omega_m^2 m^2 + \omega_s^2 s^2 + 2\omega_l\omega_m \cos(d_l - d_m) lm + 2\omega_s\omega_l \cos(d_s - d_l) sl + 2\omega_m\omega_s \cos(d_m - d_s) ms$$

or

$$P^2 = (l, m, s)\mathbf{Q}(l, m, s)^t$$

where

$$\mathbf{Q} = \begin{bmatrix} \omega_l^2 & \omega_l\omega_m \cos(d_l - d_m) & \omega_s\omega_l \cos(d_s - d_l) \\ \omega_l\omega_m \cos(d_l - d_m) & \omega_m^2 & \omega_m\omega_s \cos(d_m - d_s) \\ \omega_s\omega_l \cos(d_s - d_l) & \omega_m\omega_s \cos(d_m - d_s) & \omega_s^2 \end{bmatrix}.$$

The motion strength P is the square root of a quadratic form in the variables l, m, and s. The matrix Q is symmetric and positive semi-definite; it is positive definite if the delays d_l, d_m, and d_s are distinct.

Now consider a set of iso-motion stimuli $\{(l_i, m_i, s_i)\}$ that all generate a unit motion signal (the absolute scale of the signal is unimportant). These are described by the equation

$$(l_i, m_i, s_i)\mathbf{Q}(l_i, m_i, s_i)^t = 1$$

which is the equation for an ellipsoid.

Note that in the special case where $d_l = d_m = d_s$ (no relative delay between receptor signals) each cosine term is 1 and the expression for P simplifies to :

$$P = |\omega_l l + \omega_m m + \omega_s s|$$

which is just the monochromatic model we have rejected.

Estimating the relative L and M signal delay. In the case of stimuli without an S cone component, we can simplify the motion signal:

$$P^2 = \omega_l^2 l^2 + 2\omega_l\omega_m \cos(d_l - d_m) lm + \omega_m^2 m^2$$

$$= al^2 + blm + cm^2$$

where $a = \omega_l^2$, $b = \omega_l\omega_m \cos(d_l - d_m)$, and $c = \omega_m^2$. To fit the data in Fig. 3 with elliptical contours, we find the parameter estimates $\hat{a}$, $\hat{b}$, and $\hat{c}$ that minimize the squared deviations from the model in which all the plotted stimulus vectors generate unit motion signal:

$$\sum_i \left(1 - \sqrt{\hat{a}l_i^2 + \hat{b}l_i m_i + \hat{c}m_i^2}\right)^2.$$

From these parameter estimates, we calculate the relative delay $|d_l - d_m|$ between the L and M cones by observing that:

$$|d_l - d_m| = \cos^{-1}\sqrt{b^2/4ac}.$$

We estimate delays of 46, 118, and 154 msec between the L and M cone signals for our three observers.

Linear combination of delayed color channels

Ellipsoidal iso-motion contours. Suppose the motion strength is the amplitude of the sum of delayed signals in three color channels, each of which is a linear combination of receptor signals. Then the iso-motion contours plotted in receptor coordinates are also ellipsoidal.

Define the color channels x, y, and z as

$$(x, y, z)^t = \mathbf{T}(l, m, s)^t$$

where $\mathbf{T}$ is an invertible 3×3 matrix. Writing the delay matrix $\mathbf{R}$ for the color channels analogous to $\mathbf{Q}$ above, iso-motion stimuli (x, y, z) are described by a quadratic form:

$$P^2 = (x, y, z)\mathbf{R}(x, y, z)^t.$$

Expressing this in terms of the receptor signals,

$$P^2 = (l, m, s)\ (\mathbf{TRT}^t)\ (l, m, s)^t.$$

Since $\mathbf{T}$ is invertible, and $\mathbf{R}$ is symmetric and positive definite, $\mathbf{TRT}^t$ is symmetric and positive definite. Hence this model predicts iso-motion contours that are ellipsoidal when plotted in terms of receptor signals.

Delays confounded with choice of color channels. We now demonstrate that choice of delays is confounded with the choice of color transformation. Specifically, for any set of distinct delays, we can choose a color transformation to account for the data.

From the previous section, we know the data fall near the ellipsoid defined by the matrix $\mathbf{Q}$:

$$(l, m, s)\mathbf{Q}(l, m, s)^t = 1.$$

Choose three arbitrary distinct delays d_x,d_y, and d_z, and construct the corresponding delay matrix

$$\mathbf{R} = \begin{bmatrix} 1 & \cos(d_x - d_y) & \cos(d_z - d_x) \\ \cos(d_x - d_y) & 1 & \cos(d_y - d_z) \\ \cos(d_z - d_x) & \cos(d_y - d_z) & 1 \end{bmatrix}.$$

We construct the color transformation, $\mathbf{T}$, as follows. Since $\mathbf{Q}$ and $\mathbf{R}$ are symmetric and positive definite, we can write $\mathbf{Q} = \mathbf{U}^t\mathbf{U}$ and $\mathbf{R} = \mathbf{W}^t\mathbf{W}$, where $\mathbf{U}$ and $\mathbf{W}$ are invertible because the delays are distinct. Let $\mathbf{T} = \mathbf{W}^{-1}\mathbf{U}$, so that the color channels are

$$(x, y, z)^t = \mathbf{T}(l, m, s)^t = \mathbf{W}^{-1}\mathbf{U}(l, m, s)^t.$$

Now, the ellipsoid predicted using the delayed color channels is

$$(x, y, z)\mathbf{R}(x, y, z)^t = 1.$$

This is identical to the original ellipsoidal description of the data, since

$$\begin{aligned}(x, y, z)\mathbf{R}(x, y, z)^t &= (l, m, s)\mathbf{T}^t\mathbf{RT}(l, m, s)^t \\ &= (l, m, s)(\mathbf{W}^{-1}\mathbf{U})^t(\mathbf{W}^t\mathbf{W})(\mathbf{W}^{-1}\mathbf{U})(l, m, s)^t \\ &= (l, m, s)\mathbf{U}^t\mathbf{U}(l, m, s)^t \\ &= (l, m, s)\mathbf{Q}(l, m, s)^t.\end{aligned}$$

Since we selected the delays arbitrarily and derived corresponding color channels that describe the data, the delays in the model are confounded with the choice of color channels.

Sum of motion energy in three color channels

We now examine a model in which motion strength is the sum of motion energy in three color channels. We show that this model also predicts ellipsoidal motion nulling contours.

Since this model is nonlinear, we need to consider the net motion signal arising from the superimposed test and nulling gratings simultaneously. We represent the rightward drifting grating as a color vector $\mathbf{s}^R = (s_1^R, s_2^R, s_3^R)$ and the leftward drifting grating as $\mathbf{s}^L = (s_1^L, s_2^L, s_3^L)$. These color vectors refer to the amplitudes of the stimuli in each of the three color channels. Each color channel is some linear combination of cone signals. For example, the space–time stimulus seen by the first color channel in response to the rightward stimulus is $s_1^R \sin(x + t)$.

We postulate symmetric rightward and leftward preferring motion energy operators L_i, and R_i in the ith color channel. These sum to give the leftward and rightward motion signals L and R respectively. Motion energy operators (Adelson & Bergen, 1985) sum the squared responses of pairs of quadrature phase spatio-temporal linear operators (Fahle & Poggio, 1981; Watson & Ahumada, 1983, 1985; Adelson & Bergen, 1985; Burr, 1986). We refer to the underlying linear operators for L_i as L_i^0 amd L_i^{90}, and those for R_i as R_i^0 and R_i^{90}.

The motion nulling condition is that the leftward and rightward motion energy signals arising from the superposition of the leftward and rightward gratings cancel:

$$L(\mathbf{s}^R + \mathbf{s}^L) = R(\mathbf{s}^R + \mathbf{s}^L).$$

For simplicity (and without loss of generality) we assume that the stimuli begin in the same spatial phase. Then we can write the responses of the leftward-preferring linear operators to the leftward and rightward gratings as:

$$\begin{aligned} L_i^0(\mathbf{s}^L) &= \omega_i^p s_i^L \sin(t) \\ L_i^0(\mathbf{s}^R) &= \omega_i^o s_i^R \sin(t) \\ L_i^{90}(\mathbf{s}^L) &= \omega_i^p s_i^L \cos(t) \\ L_i^{90}(\mathbf{s}^R) &= \omega_i^o s_i^R \cos(t) \end{aligned}$$

where ω_i^p and ω_i^o are the sensitivities of L_i^0 and L_i^{90} to gratings of unit spatial and temporal frequencies moving in the (p)referred and (o)pposite directions. The direction preference is expressed in the relation $|\omega_i^p| > |\omega_i^o|$. Since R_i^0 and R_i^{90} are symmetric to L_i^0 and L_i^{90}, an almost identical set of equations governs their responses, with ω_i^p and ω_i^o interchanged.

The leftward motion signal is given by the sum of the leftward-preferring energy operators, which in turn sum the squared outputs of the underlying linear operators:

$$\begin{aligned} L(\mathbf{s}^L + \mathbf{s}^R) &= \sum_i L_i(\mathbf{s}^L + \mathbf{s}^R) \\ &= \sum_i [L_i^0(\mathbf{s}^L + \mathbf{s}^R)]^2 + [L_i^{90}(\mathbf{s}^L + \mathbf{s}^R)]^2 \\ &= \sum_i [L_i^0(\mathbf{s}^L) + L_i^0(\mathbf{s}^R)]^2 + [L_i^{90}(\mathbf{s}^L) + L_i^{90}(\mathbf{s}^R)]^2 \\ &= \sum_i (\omega_i^p s_i^L + \omega_i^o s_i^R)^2(\sin^2(t) + \cos^2(t)) \\ &= \sum_i (\omega_i^p s_i^L + \omega_i^o s_i^R)^2. \end{aligned}$$

Similarly,

$$R(\mathbf{s}^R + \mathbf{s}^L) = \sum_i (\omega_i^p s_s^R + \omega_i^o s_i^L)^2.$$

We now show that the iso-motion contours are ellipsoidal. Suppose that the leftward stimulus is the test stimulus; it is described by a fixed color vector $\mathbf{s}^L$. We seek the stimuli $\mathbf{s}^R$ that satisfy the nulling condition

$$L(\mathbf{s}^R + \mathbf{s}^L) = R(\mathbf{s}^R + \mathbf{s}^L).$$

Substituting the expressions for L and R above, we have

$$\sum_i (\omega_i^p s_i^L + \omega_i^o s_i^R)^2 = \sum_i (\omega_i^p s_i^R + \omega_i^o s_i^L)^2.$$

Expanding and rearranging,

$$\sum_i [(\omega_i^p)^2 - (\omega_i^o)^2](s_i^R)^2 = \sum_i [(\omega_i^p)^2 - (\omega_i^o)^2](s_i^L)^2.$$

Since the test stimulus $\mathbf{s}^L = (s_1^L, s_2^L, s_3^L)$ is fixed, we can write the right hand side as a constant k. Note that $k > 0$ since $|\omega_i^p| > |\omega_i^o|$ (excluding the case $\mathbf{s}^L = 0$). Similarly, the constant $a_i = [(\omega_i^p)^2 - (\omega_i^o)^2]/k$ is positive. Therefore the iso-motion stimuli $\mathbf{s}^R = (s_1^R, s_2^R, s_3^R)$ lie on an ellipsoid defined by the equation

$$\sum_i a_i (s_i^R)^2 = 1.$$